A point-by-point response to the reviews

Response to the first reviewer's comments

General comments:

This manuscript, AMT-2020-94, reports the evaluation of new O3 xsec data sets (labeled as "BW") measured in the Hartley and Huggins bands for the use of O3 profile retrieval from OMI observations. The BW data sets were modeled by using a polynomial in a function of temperature in order to facilitate direct comparison with the current reference data set ("BDM") and their application to the O3 profile retrieval. They have found that the new data set, BW, shows a better performance in the retrieval of O3 profile in terms of less oscillatory features in the retrieved profile and better agreement with the ozonesonde data. We found the manuscript written in a nice and compact manner; the presentation looks consistent. However, we are not convinced that we can agree with the authors' the interpretation of what is described in Sec. 2, which will be detailed below.

This manuscript has shown well that the new dataset, BW, is better than the BDM in the O3 profile retrievals primarily because of their wider temperature coverage, esp. going down to 194
K critical to the retrievals in the transition layers (UTLS), which was not covered by the BDM dataset in temperature. Therefore, the conclusion of this work has been supported by the results presented in the manuscript. The topics of this paper highly relevant to the scope of AMT, so that we recommend a publication of this manuscript to AMT with a revision or a further clarification
Sec. 2. Specific comments and suggestions follow.

Responses to general comments

We would like to thank this reviewer for the constructive comments. We did our best to sincerely reply to 4 comments made by this reviewer.

Specific comments

C1. The authors wrote "Offset corrections were made for each of the 6 temperatures by fitting to the SER dataset since it was measured at higher ozone column density and thus considered more reliable regarding offset". Does this mean that the BW xsec was normalized to that of SER. Clarify what the corrections factors were and how (and what wavelengths) they were determined. Was this offset considered in the error budgets?

R1. Offset errors in the baseline of the measured spectra cause offset errors in the absorption cross section. Since the column amount of the ozone was limited by the relatively small absorption path of 22.1, the offset error in the ACS was relatively large, up to 2e-22 cm^2/molec. Around 344 nm this amounts to about 20% of the ACS. At 330 nm the offset is about 4%. At 270 nm the offset is about 0.0025%. In order to correct this error fits of the BW ACS to the SER ACS fitting a scalar and an offset were performed in the range 317-350 nm. The offset error in the SER ACS were much smaller due to the significantly longer absorption path (270 cm). The scalar was ignored. The offset was used to correct the entire wavelength range, but it would not have made a difference if we had limited it to the fit range since the offset error influence below 330 nm is negligible. The offset uncertainty was determined from the standard deviation of the fit multiplied with chi since the residuals were not purely noise. The offset uncertainty was 1e-24 cm^2/molec, which is negligible. We think that this discussion is beyond the scope of this paper, which is not intended, for developing/introducing this spectroscopic data, but for applying this dataset on our retrievals. The related discussion will be addressed in a separate paper lead by the author of this dataset, Manfred Birk.

C2. Author wrote, "After offset correction polynominals of 1st order (<270.27 nm) and 2nd order (>270.27 nm) in temperature were fitted for each spectral point to improve the statistical uncertainty" and followed by "Measured cross-sections are typically parameterized quadratically to be applied conveniently at any atmospheric temperatures" using the following equation: $C = C_o + C_1(T - 273.15) - C_2(T - 273.15)^2$.

C2-1. The agreement between the original data and the fitted data should be inspected or discussed for each of the two data sets, BW and BDM, and discussed. Besides, direct comparison of their original data sets between BW and BDM (prior to having them fitted to the polynomial), which may be done at T = 273 and 295 K provided that their temperature differences, $\Delta = 0.5$ and 0.7K, respectively, is insignificant, which seems true because the authors argued the dominant coefficient C0 is almost independent of temperature.

R2-1. As mentioned in Section 2, the temperature correction has already been applied in the BW dataset available to the public. This paper is devoted to atmospheric validation of the BW dataset, rather than presenting the data det itself. We think that it is out of scope to give a detailed evaluation for the original BW dataset where either offset and temperature correction is turn off because it is not officially published. The detailed views on the original/corrected BW dataset will be provided in another paper written by Birk and Wagner. In the ozone profile algorithm the cross sections parameterized using this quadratic equation are typically used to represent the dependence of cross-section on the atmospheric temperature vertically rather than the interpolated spectrum from original measurements. Therefore, this paper focused on comparing coefficients and the parameterized cross-sections between BDM and BW datasets.

C2-2. We are not sure how well the Eq. (1) could have captured the temperature dependence of the xsec. The xsec can be represented by integrated (line) intensities for the given frequency (wavelength) grid, and the temperature dependence of the line intensities can be modeled by two
parameters, i.e., partition function (which we know well for O3) and the lower state energies (which we do not know for the features of this work). Thus, one can simulate the intensity ratio to that at 296 K at various temperature for a few representative cases of the lower state energies, as shown in Fig. X below. As we see, Fig. X is similar to the right panel of Fig. 1, except for one thing that each curve in Fig. X represents different values of the lower state energies, not the wavelength presented in Fig. 1. There is a possibility of having the sampled wavelengths (such as 280, 290,..., in nm) possessing progressively higher value of their (effective) lower state energies more appropriate to assume that each curve in Fig. 1 corresponds to a different of multiple transitions falling into the particular wavelength data point grid (for instance, 280nm±resolution element). This point should be addressed properly to keep naive readers from being misled to think the temperature dependences in Fig. 1 is attributed to the wavelengths.

R2-2. The quadratic equation was first found to represent well the temperature dependence of ozone cross sections in the UV [Paur and Bass, 1985] and has now become the standard approach [Liu et al., 2007;2013; Chehade et al., 2013a,b; Serdyuchenko et al., 2014]. In addition, Fig. X (this reviewer plotted) and Fig. 1 in this paper commonly imply that the dependence of the cross-section on the temperature tends to be linear at shorter wavelengths and slightly non-linear at longer UV wavelengths. Therefore, the quadratic (2nd) polynomials seem to be adequately fit the cross-section measurements. In revised manuscript, this discussion has been better specified by adding "This quadratic equation was first found to represent well the temperature dependence of ozone cross section in the UV (Paur and Bass, 1985) and has now become the standard approach (Liu et al., 2007; 2013; Chehade et al., 2013a;2013b; Serdyuchenko et al., 2014)" after the equation 1.
The approach suggested by the reviewers is somewhat similar to pseudolines that is sometimes employed in the parametrizing the IR cross-sections, where temperature and presuure-dependent cross-sections are fit to a HITRAN-like line list where "transitions" do not have quantum mechanical meaning but do reproduce cross-sections. However, this approach is a lot more sophisticated than suggested by the reviewers because

there are more than one transitions (with different intensities and lower state energies) that underlie absorption at selected wavelength. This very non-trivial and intense task has never been applied to the electronic spectra yet.

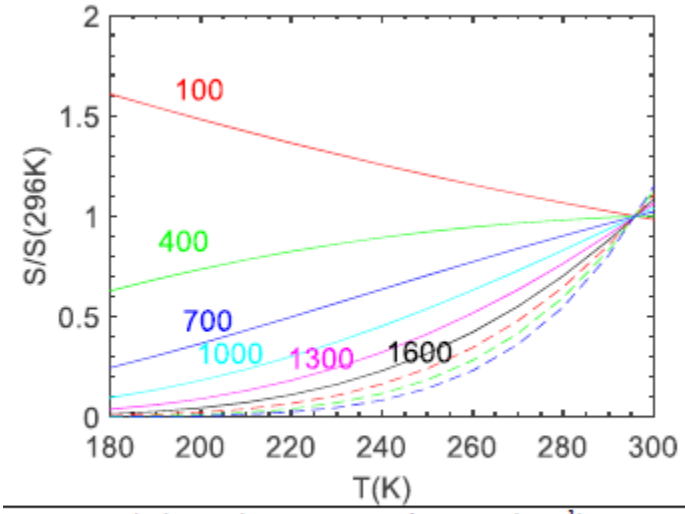

Fig. X S/S(296K) vs. T at a given E"(cm^{-1}) =[100,400,700,1000, 1300, etc.]

C2-3 For the same reason, Fig. 2 is hard to interpret. The respective comparison of the C1 and C2 for two different data set as a function of nm could be legitimate only when the two data sets are measured at the same resolution because the effective lower state energies mentioned above would be the same. Therefore, the non-wavy feature of C2 for the BW data set would have more to do with the outcome of the resolution choice in the representation by Eq.(1), rather than it is telling the BW data set is superior to the BDM dataset in the temperature consistency. In other words, Fig. 2 shows which data set is better represented by Eq. 1 rather than which data is closer to the truth. This section may stay, but with a specific statement, being provided for the readers on the point made above. The bottom line is that the BW data set is better than the BDM set because of the broader coverage of the measurement temperature, especially covering the temperature critical to UTLS layers, as was properly concluded by the authors in the manuscript.

R2-3. We agree with this comment; it could be not straightforward to compare the coefficients especially C1 and C2 derived from BDM and BW, respectively, due to different spectral resolutions and the strong correlation between C1 and C2 especially when the temperature dependence is weak. However, important insights are obtained from this figure; the comparison of C_o indicates systematic biases between two datasets, by 2 % on average, with some spikes of up to 8 % at longer UV wavelengths above 315 nm mainly due to the different spectral resolution. The C_1/C_2 characterizes the linear/non-linear dependence of the cross-sections. As shown in Figure 3.c, the quadratic temperature dependence show different behaviors in 290-310 nm, which is significantly correlated with the comparison of cross-section spectrum shown in Figure 4.

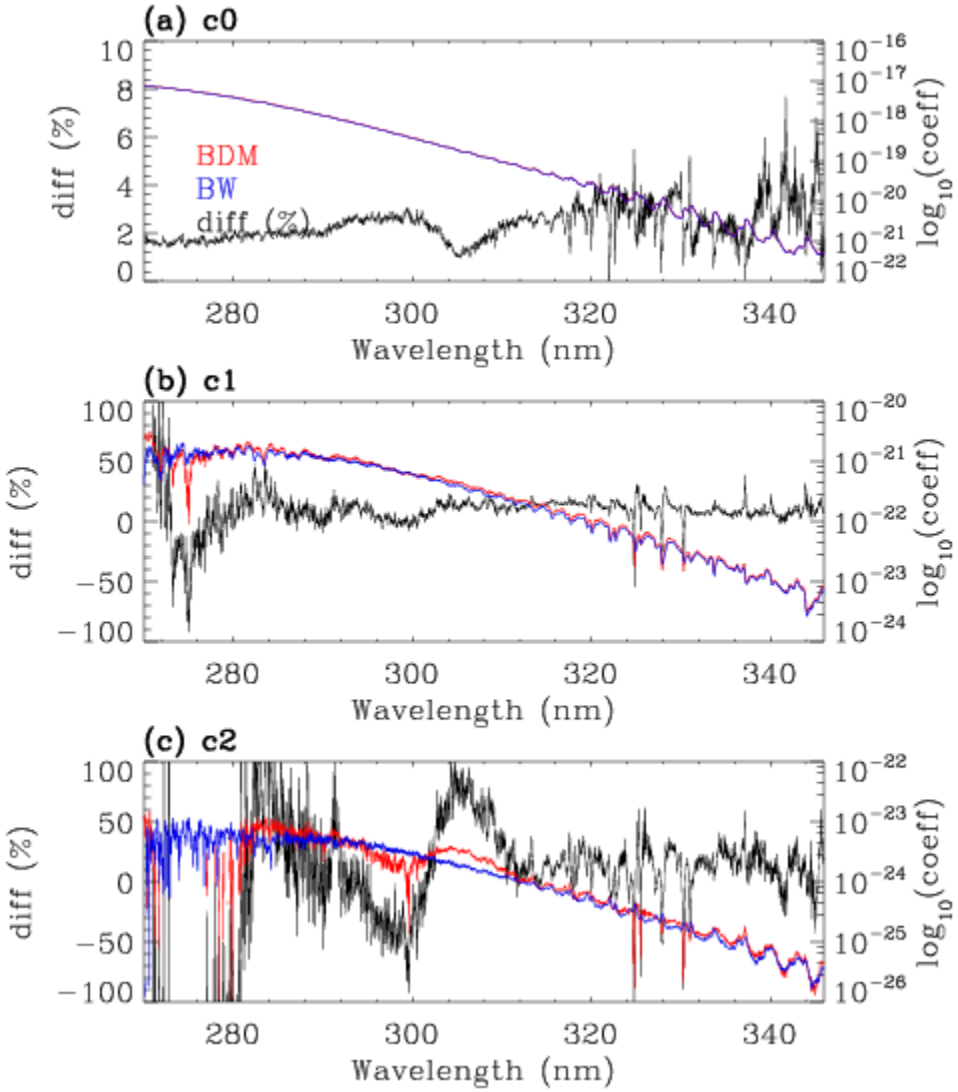

Revised Figure 4.

Response to the second reviewer's comments

General comments:

The manuscript AMT-2020-94 provides a comparison of UV ozone retrievals from the OMI instrument using a new cross section data set (BW, provided in the frame of the ESA SEOM-IAS project) with the standard data set from Reims (BDM). Overall, the manuscript is very well written, nicely structured and argued. Selected figures do well illustrate the discussion in the manuscript. The presentation is scientifically sound and clear. The topic fits nicely within the journal scope and, therefore, I can fully recommend publishing the manuscript. There are a few issues to the current paper that need to be addressed before publication, however.

Responses to general comments

We would like to thank this reviewer for the constructive comments. All the comments made by this reviewer were addressed in the revised manuscript.

C1. The analysis is based on a new cross section data set (BW data) that at this point of time is openly available, but has not yet been published in the scientific literature. It therefore lacks yet the scrutiny of the peer-review process. While this is a regrettable fact, it does not invalidate the present work. But the authors must carefully discuss what might possibly be an inherent contradiction. In a previous study (Liu et al., 2013), the authors have concluded that another recent UV cross-section data set (the SER data from Bremen, Serdyuchenko et al. (2014); Gorshelev et al. (2014)) was less suited for ozone retrievals using the OMI-spectrometer than the BDM data, despite a similar spectral resolution (0.01nm − 0.018nm for the 210 − 350nm range) and a much better temperature coverage (data between 193 K and 293 K on a grid of 10 K; see Weber et al. (2016) for example). Surprisingly, the same data set (SER) is now used to 'calibrate' the new BW data (see lines 95-99 of the manuscript): Offset corrections were made for each of the 6 temperatures by fitting to the SER dataset since it was measured at higher ozone column density and thus considered more reliable regarding offset. The offset corrections have minor effect on the cross-sections except for wavelengths above 330 nm. The procedure of dismissing the SER data set for ozone retrieval, but using it for calibration is confusing and needs further explanation. The calibration procedure is even more surprising as the correction actually does not seem to impact the results of the present paper, because corrections are claimed to have minor effects within the OMI windows (>330 nm). The necessity of making an offset correction arises from the measurement technique/setup at DLR. It thus needs to be explained why there is the need to make an offset correction in the first place and why the SER data do not suffer from the same problem.

R1. Offset errors in the baseline of the measured spectra cause offset errors in the absorption cross section. Since the column amount of the ozone was limited by the relatively small absorption path of 22.1 cm the offset error in the ACS was relatively large, up to 2e-22 cm^2/molec. Around 344 nm this amounts to about 20% of the ACS. At 330 nm the offset is about 4%. At 270 nm the offset is about 0.0025%. In order to correct this error fits of the BW ACS to the SER ACS fitting a scalar and an offset were performed in the range 317-350 nm. The offset error in the SER ACS were much smaller due to the significantly longer absorption path (270 cm). The scalar was ignored. The offset was used to correct the entire wavelength range, but it would not have made a difference if we had limited it to the fit range since the offset error influence below 330 nm is negligible. The SER data used for the offset fit were at longer wavelength and measured with an FTS, too. The structure of the spectra in this region agreed well beside a scalar up to 1.03, depending on temperature. In the lower wavelength range the SER data were obtained using a grating spectrometer and there were distinct differences in the structure. The offset correction is only relevant when using ACS at longer wavelength (e.g. Brewer, Dobson). In the current paper, however, opaque regions at lower wavelength are of interest, where the impact of the offset is rather small. As addressed to the answer to comment 1 from the first review, this discussion is out of scope to be detailed in this paper.

C2. In the introduction, the authors give the impression that new cross sections should be measured at a resolution of 0.01nm or better. This contradicts the use of new cross section data that have been obtained at about 3 (> 285.7 nm) to 5 (< 285.7 nm) times lower resolution (see description of BW data set in section 2).

The spectral resolution requirement is from Orphal et al. (2016): ozone cross-sections should be measured at high spectral resolutions (typically 0.01 nm in the ultraviolet-visible). So the citation of "a resoultion of 0.01 nm or better" is not accurate and is probably confused with the wavelength calibration requirement "the spectral wavelength) calibration must be very accurate, too (typically at least 0.01 nm). For the BW dataset, measurements are performed at a coarser resolution to cover the broad spectral range as a tradeoff or spectrally degraded in the post-processing to increase signal to noise ratio. Indeed, the spectral resolution of 3.3 cm^{-1} may have caused a very small deterioration of the highly resolved spectral features occurring above 325 nm. The high resolution structures have only a very small contrast regarding the underlying broad features. The impact is expected to be small, especially in view of the low resolution of the remote sensing instruments.

C3. The authors use the terms Hartley and Huggins bands as well as OMI instrument windows to discuss different spectral regions in the UV. While wavelength ranges for both of the OMI UV windows are specified in the manuscript, no numbers are given for the Hartley and Huggins bands. Please indicate as this would help readers to follow the discussion.

R3. We has specified the bands in the revised manuscript where these bands are first mentioned such as "C_o values are similar to each other in the Hartley band (< 310 nm) with relative biases of 2-3%. However, the Huggins band (> 310 nm) shows large spiky biases of up to 8%. C_1 and C_2 represent linear and quadratic temperature dependences of absorption cross-sections, respectively"

C4. There seem to be problems with the definitions of signs in some of the plots. For example, are the signs in Figure 7 correct? I find that local negative spikes in the total ozone column difference (BDM-BW) also correlate with cases where the tropospheric profile shows a tendency towards warmer colors (BDM > BW), which would indicate that either of the two scales (total ozone (TOC) vs altitude dependent ozone) should have a different sign. Another issue is the Antarctic +1%BDM-BW bias in the TOC. From Figure 4, one would estimate that the cross section bias is positive when integrated all over the $(270-346)$ nm wavelength range (despite some few local negative spikes at low temperatures). This should result in a negative BDM-BW bias of TOC. Anyway, the antarctic positive TOC bias needs to be discussed as compared to the lower latitude value around −1% on the basis of the cross section data. In similar veins, the definition of the y-axis of Figure 4 shows that the room temperature BW cross-section is negatively biased with respect to BDM at low wavelengths. This is opposite to what is stated in line 254 of the manuscript (Relative to the BDM data set, the BW data show systematic biases of 2−3% in C0 at shorter wavelengths below 300 nm).

R4. The contour map gives an impression that applying BDM causes the overestimation, especially around the tropopause where the coldest temperature/the lowest ozone amount is found. The impact of applying different cross-section dataset on total ozone retrievals are overwhelmed mainly by the lower stratospheric layers where the ozone amount is relatively large and the dependence of ozone-cross sections on the temperature is relatively important. Please take a look at the revised Figure 7 also including the contour map for absolute differences in the unit of DU (Figure 7.b), which shows that applying BDM causes the significant negative biases in the lower stratosphere (20-30 km) and then total ozone columns are underestimated. On the other hand, the BDM based total ozone columns are overestimated in South Pole due to the biggest inconsistency of two cross-sections at the coldest temperatures just above the tropopause. In the revised manuscript, this part has been better specified in page 6 as following:

Figure 7 shows both relative and absolute differences of the retrieved ozone profiles with the corresponding temperature profiles taken from the National Centers for Environmental Protection (NCEP) final (FNL) operational global analysis data. Large differences of 20-50% commonly exist along the tropopause, where

the original BDM measurements could not cover atmospheric temperatures below 218 K (Fig. 7a). Some larger differences occur throughout the troposphere in the tropics likely due to the relative smaller retrieved partial ozone columns. The individual differences of retrieved ozone in the lower troposphere are ~ 20%. However, the corresponding impact on the total column ozone, from integrating retrieved ozone profiles are overwhelmed by the stratospheric layers (20-30 km), as shown in Fig. 7b, where the ozone amount is relatively large and the dependence of ozone-cross sections on the temperature is still important. As a result, applying BDM causes an underestimation of total ozone except at the South Pole due to the biggest inconsistency of two cross-sections at the coldest temperature just above the tropopause in spite of smaller amount of ozone compared to upper stratospheric layers. The magnitude of this underestimation/overestimation is ~1 %, which is comparable to the overall accuracy (~1.5%) of the OMI operational total ozone product against ground-based measurements (McPeters et al., 2015).

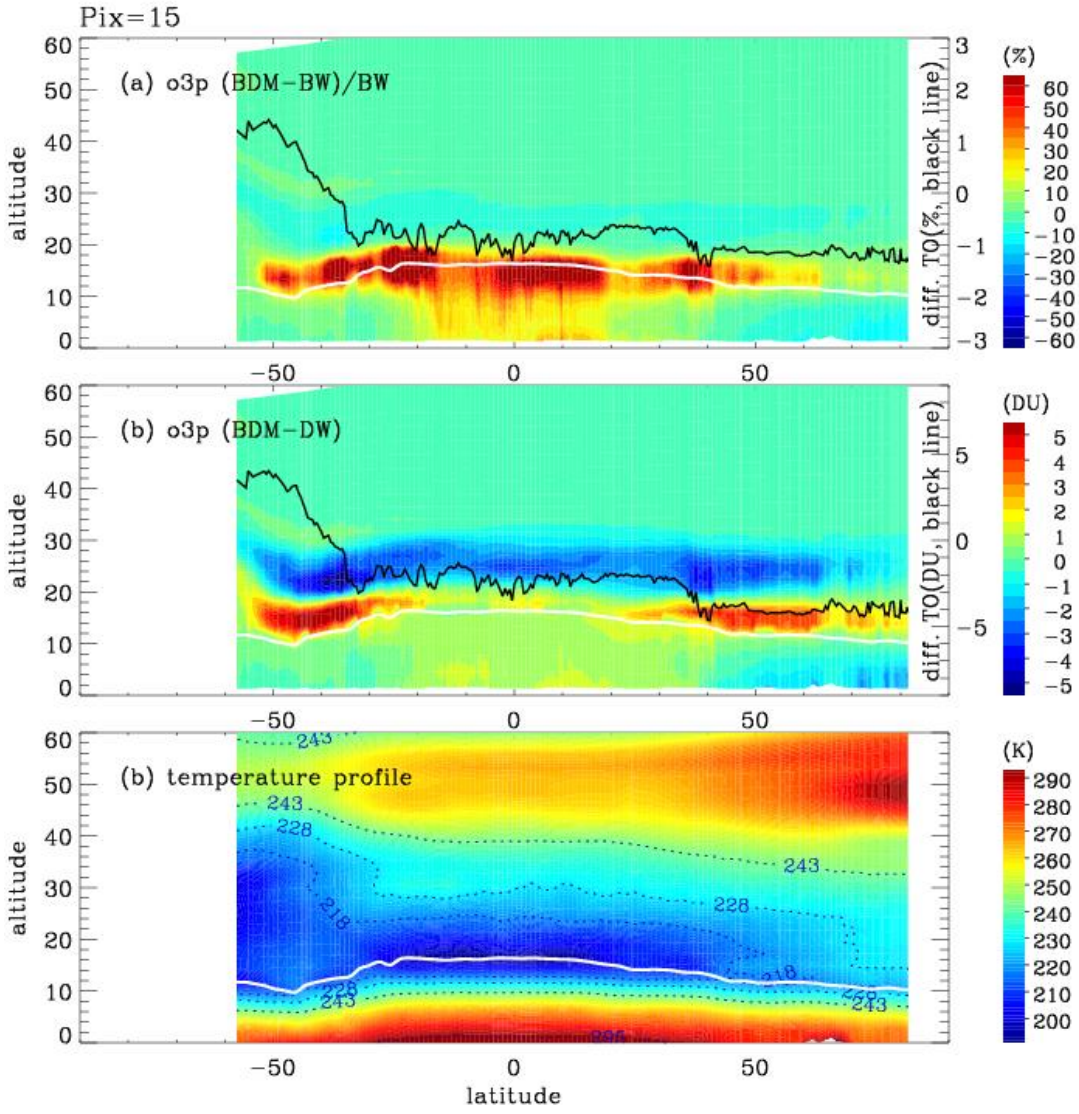

Figure 7 in the revised manuscript.

C5. In the comparison between BDM and BW in section 3, the BW data set is taken as the baseline scenario. Because section 3 only provides a relative comparison and not an accuracy assessment, the authors should avoid the impression that BW is the truth (even though it compares more favorably with ozonesonde data presented in the next section 4). Instead of saying that BDM causes an underestimation or overestimation, it should just be stated that BDM estimates are lower or higher than estimates from BW.

R5. We agree with this comment. The manuscript has been revised to reflect this suggestion.

C6. Fig. 9 shows the OMI mean biases with respect to a common reference (ozonesonde). It would be nice to plot the reference profiles (or mean profiles with their sdev) along with the bias percentages.

R6. We have revised Figure 9, according to this comment. The revised figure is following:

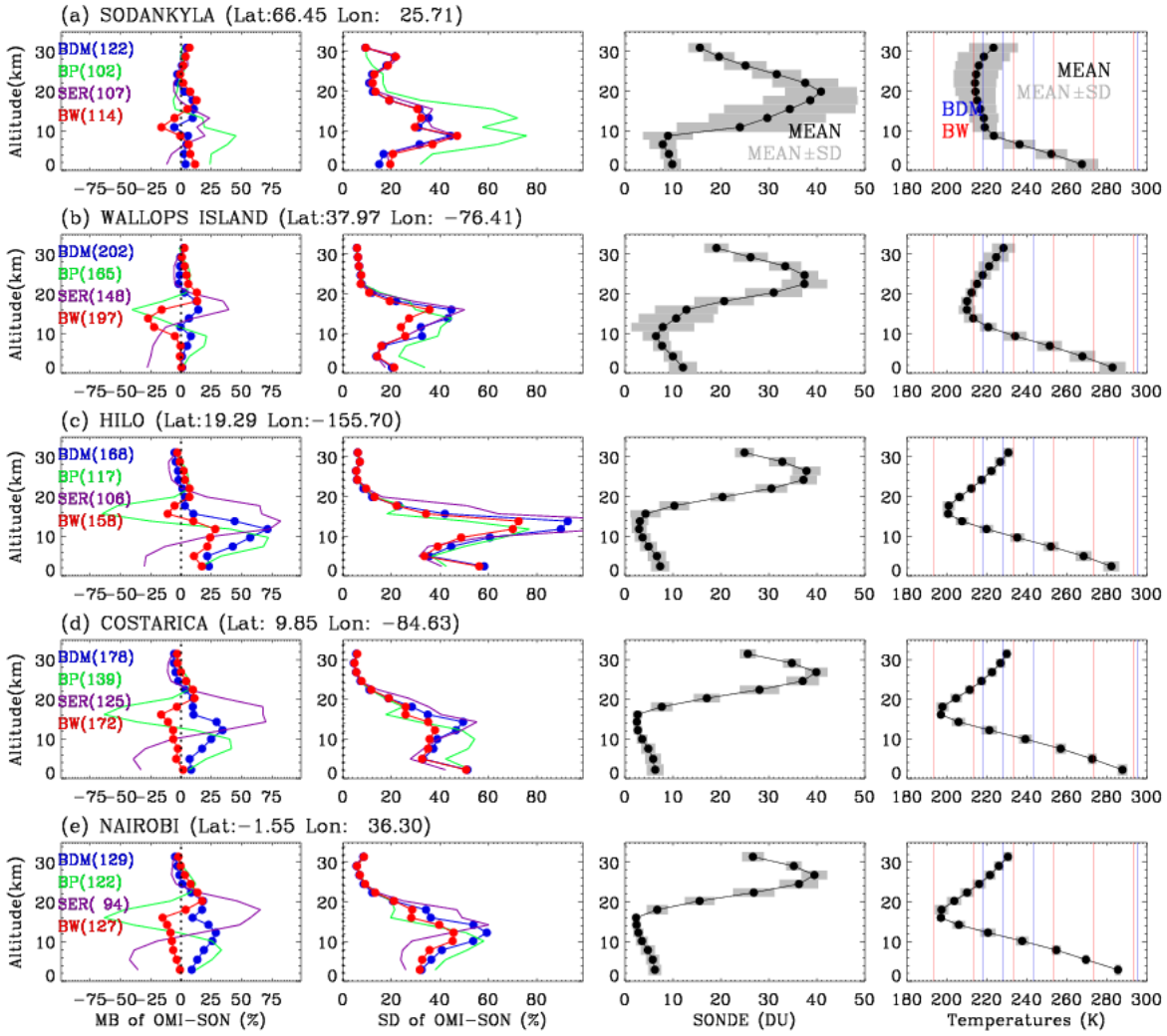

Figure 9.

C7. TEMPO is not the only mission that will critically depend on refined ozone spectral data. IASI NG and UVNS are another example of combining retrievals in different domains. In the discussion, the authors need to mention/cite other ongoing or future activities on the synergistic use of different spectral regions that rely on the 9.6 μm region and the Chappuis band, eg. Costantino et al. (2017) and/or others.

R7. Yes, there are many on-going projects requiring the advanced ozone spectral data. However, the ozone profile algorithm used in this paper is optimized to retrieve ozone profiles from OMI BUV measurements with the capability of processing GOME, OMPS, and GOME/2 measurements, commonly focusing on the Hartley and Huggins bands. Furthermore, the TEMPO ozone profile algorithm has been under development by extending this OMI algorithm from UV only to UV+Visible. There have been several studies including this paper to recommend the reference ozone spectral data for UV spectral fitting, but nothing for the Chappuis band. Therefore, in the last section of this paper we addressed the importance about evaluating the visible ozone cross-section datasets, focusing on the SER and BDM datasets, which is one of priorities in the development of the TEMPO ozone profile algorithm. In this context, we think that it is out of scope to address other missions employing the thermal IR.

2. Technical

C1. (L32) th → the
R1. It has been revised.

C2. (L95) indicate whether offset was assumed to be constant or wavelength dependent
(for wavelength dependent offset specify dependence and range)
R2. The associated sentence has been revised for clarification from "Offset corrections were made for each of the 6 temperatures by fitting to the SER dataset" to "Offset corrections were made for each of the 6 temperatures by fitting to the SER dataset (constant for all wavelengths)"

C2. (L97) (<270.27 nm) > and → (<270.27 nm) and
C3. (L106) temperatures → temperature
C4. (L107) Should use terms (T − 273.15K) and (T − 273.15K)2 including the unit of K in eq. (1).
C5. (L170) 0.015 in UV1 → 0.015nm in UV1
C6. (L254) BW data show systematic biases of 2-3% in C_0 → BW data show systematic biases of 2-3% in the cross section at O°C (C_0)
C7. (L255) The difference in C1 and C2 implies distcinctly different → The differences in C1 and C2 imply a distinctly different
C8. (L268) 200K → 200 K
C9. (L355) list all author names
C10. (L364) J. Quant. Spectrosc. Ra. → J. Quant. Spectrosc. Radiat. Transfer
R2-R10. We accepted all these suggestions.

C11 (p. 15) Panels (a) - (c) should use logarithmic scales for the coefficients as BDM and BW curves are indistinguishable from 0 at wavelengths ≥ 325 nm.
R12. We revised Figure 2 to use logarithmic scales in y-axis.

C12 (p. 16) Legend to Figure 3 should contain hint on the factor of five different scales used in panels (a) and (b).
R12. In caption, it was detailed like "In the legend, the temperatures not covered by each dataset are indicated with gray and black, for values beyond lower and upper boundaries, respectively", but we added "T > T^{BDM}_{max} T< T^{BDM}_{min}" in Fig. 3 a and "T > T^{BW}_{max} T< T^{BW}_{min} in Fig. 3. b according to this comment.

C13 (p. 17) Legend to Figure 5 should better describe what is on the plot.
R13. For clarification, the caption has been revised like "The impact of parameterizing the cross-sections shown in Figure 3 on ozone profile retrievals, for (a) BDM and (b) BW, as a function of solar zenith angle

(SZA). The differences of retrieved ozone profiles are assessed in absolute (left panels) and relative (right panels) units, respectively."

C14 (p. 19) & 22 Degree symbol ° before K in x-axis legend of Figure 9 needs to be deleted.
The same holds for the lower colour legend in Figure 7.
R14. °K has been corrected to K in indicated figures.

C15 (p. 21) Annotations MB and MB ± SD in upper right panel are misleading (there is no mean bias in the temperature plot). The 294 K temperature line for the BDM temperature point is drawn differently (thicker, other colour) than the other temperature lines.
R15. This figure has been replotted after correcting indicated annotations and line.

- List of the revised figures : 2, 3, 7, 9, 10

Impact of using a new ultraviolet ozone absorption cross-section dataset on OMI ozone profile retrievals

Juseon Bak[1], Xiong Liu[1], Manfred Birk[2], Georg Wagner[2], Iouli E. Gordon[1], and Kelly Chance[1]

[1]Harvard-Smithsonian Center for Astrophysics, Cambridge, MA, USA

[2]Deutsches Zentrum für Luft- und Raumfahrt e.V. (DLR), Remote Sensing Technology Institute, Oberpfaffenhofen, D-82234 Wessling, Germany

Abstract

We evaluate different sets of high-resolution ozone absorption cross-section data for use in atmospheric ozone profile measurements in the Hartley and Huggins bands with a particular focus on Brion-Daumont-Malicet et al. (1995) (BDM), currently used in our retrievals, and a new laboratory dataset by Birk and Wagner (BW) (2018). The BDM cross-section data have been recommended to use for retrieval of ozone profiles using spaceborne nadir viewing Backscattered UltraViolet (BUV) measurements since its improved performance was demonstrated against other cross-sections including Bass and Paur (1985) (BP) and those of Serdyuchenko et al (2014) and Gorshelev et al. (2014) (SER) by the "Absorption Cross-Sections of Ozone" (ACSO) activity. The BW laboratory data were recently measured within the framework of the ESA project SEOM-IAS (Scientific Exploitation of Operational Missions - Improved Atmospheric

Spectroscopy Databases) to provide an advanced absorption cross-section database. The BW cross-sections are made from measurements at more temperatures and in a wider temperature range than BDM, especially for low temperatures. ~~Compared to~~Relative differences of cross-sections between BW ~~,~~and BDM ~~cross-sections are positively biased~~range from ~2 % at shorter UV wavelengths to ~5 % at longer UV wavelengths at warm temperatures. Furthermore, these ~~biases~~ differences dynamically increase by up to ± 40 % at cold temperatures due to no BDM measurements having been made below 218 K. We evaluate the impact of using different cross-sections on ozone profile retrievals from Ozone Monitoring Instrument (OMI) measurements. Correspondingly, this impact leads to significant differences in individual ozone retrievals, by up to 50 % in the tropopause where the coldest atmospheric temperatures are~~is~~ observed. Bottom atmospheric layers illustrate the significant change of the retrieved ozone values, with ~~biases~~ differences of 20 % in low latitudes, which is not the case in high latitudes because the ozone retrievals are mainly controlled by a priori ozone information in high latitudes due to less photon penetration down to the lower troposphere. Validation with ozonesonde observations demonstrates that BW and BDM retrievals show altitude-dependent bias oscillations of similar magnitude relative to ozonesonde measurements, much smaller than those of both BP and SER retrievals. However, compared to BDM, BW retrievals show significant reduction in standard deviation, by up to 15 %, especially at the coldest atmospheric temperatures. Such improvement is achieved mainly by the better characterization of the temperature dependence of ozone absorption.

1. Introduction

Accurate knowledge of the absorption cross-sections of ozone and their temperature dependence is essential for highly accurate measurements of atmospheric ozone (Orphal et al., 2016) as well as other trace gases affected by the strong ozone absorption such as BrO, NO_2, SO_2, and CH_2O (e.g., Seo et al., 2019; Theys et al., 2017). In the laboratory, measuring ozone cross-sections which can meet the high requirements for accurate ozone profile measurements covering a wide spectral range (at least 270-340 nm) at high-resolution (typically 0.01 nm) at a wide range of atmospheric temperatures (180-300 K) ~~–~~is still challenging ~~in covering a wide spectral range (at least 270-340 nm) at high resolution (at leasttypically 0.01 nm) at a wide range of atmospheric temperatures (180-300 K)~~. The difficulties range from reactivity of ozone to calibration standards. For instance, as discussed in the recent review by Hodges et al. (2019) the accepted calibration of ozone cross-sections at the 254 nm mercury line (Hearn~~-~~, 1961) was in need of revision. In addition, simultaneous measurements of ozone in the microwave, infrared and ultraviolet regions are subject to uncertainties due to systematic differences in the respective regions (cf.~~see discussion in~~ Birk et al. (2019~~;) and~~ Tyuterev et al. (2019)~~ for instance~~). The need to evaluate existing cross-sections

used for all atmospheric measurements of ozone and to make its recommendations initiated the "Absorption Cross-Section of Ozone (ACSO) activity" that was established in 2008 and conducted in two phases (2009-2011, 2013) (Orphal et al., 2016). The ACSO activity shows the need to continue laboratory ozone cross-section measurements of highest quality.

Prior to ACSO activities, the available ultraviolet (UV) ozone-cross sections were thoroughly reviewed by Orphal (2002, 2003) and as a result three datasets of ozone cross-sections were found to be in agreement of 1-2 % with each other, including BP 1985 (Bass and Paur, 1985), BDM 1995 (Daumont et al. 1992; Brion et al., 1993; Malicet et al., 1995), and Global Ozone Monitoring Spectrometer (GOME) flight model (Burrows et al., 1999) (GMFM). The BP dataset is no longer recommended for any atmospheric ozone measurements (Orphal et al., 2016), but still used to keep the long-term consistency of ground-based Dobson/Brewer total ozone records and spaceborne TOMS/OMI total ozone records (McPeters et al. 2015). These cross-sections were also included in the 2004 edition of the HITRAN database (Rothman et al., 2005) and remained unchanged in subsequent editions including HITRAN2016 (Gordon et al., 2017). Using GMFM is restricted to GOME measurements because these cross-sections were measured at GOME resolution (~0.2 nm). On the other hand, the high-resolution cross-sections of BDM were first applied by Liu et al. (2005) for GOME ozone profile retrievals in the literature. In Liu et al. (2007), these three datasets were thoroughly assessed to find the most suitable cross-sections for GOME ozone profile retrievals (290-307 nm and 325-340 nm). As a result, they recommended using the BDM for ozone profile retrievals due to much smaller fitting residuals and better agreement with ozonesonde measurements. Such improvement is likely due to better spectral resolution and wavelength calibration of BDM than BP and GMFM. After that, the recommendation of BDM for satellite ozone profile retrievals has been officially made by the ACSO activities during the first phase (2009-2011) and the second phase (2013), respectively. The first activity was focused on the intercomparison between BDM and BP, while the second activity was additionally organized in response to the new publication of a high-resolution laboratory dataset covering the temperature range of 193 to 293 K in 10 degree step by Serdyuchenko et al. (2014) and Gorshelev et al. (2014) (abbreviated as SER). In the framework of the ACSO activity, Liu et al. (2013) evaluated the impact of changing from BDM to SER on Ozone Monitoring Instrument (OMI) ozone profile retrievals (270-330 nm). The recommendation of the BDM was made again for use in ozone profile retrievals. Recently, a new laboratory dataset was measured at the German Aerospace Center (DLR) within the framework of the ESA project SEOM-IAS (Scientific Exploitation of Operational Missions - Improved Atmospheric Spectroscopy Databases) in order to improve the atmospheric BUV retrievals from the TROPOspheric Monitoring Instrument (TROPOMI) on board the Sentinel 5-Precursor satellite (Birk and Wagner, 2018) (abbreviated as BW). A publication with more details on the experiment and analysis is in preparation. Here, we ~~This~~

~~motivates us to~~ investigate if the current recommendation ~~could~~ should be replaced with the BW dataset. This work will also help making the decision on ~~what~~ which cross-sections should replace BP measurements in the HITRAN database.

This paper is organized as follows: Section 2 compares ~~the~~ quadratic coefficients in the parameterization of temperature dependence and evaluates the parameterized cross-sections against interpolated ones. Section 3 analyzes the differences in individual OMI retrievals due to different cross-sections, which are evaluated against ozonesonde observations in Section 4. The~~is~~ paper is ~~finally~~ summarized and discussed in Section 5.

2. Comparison of BDM and BW

The BW dataset is publicly available at https://zenodo.org/record/1485588, along with ~~some~~ experimental descriptions. A detailed publication is planned to describe the details of the experimental setup and procedure so only a brief overview is given here. These cross-sections are given at six temperatures (193, 203, 233, 253, 273, and 293 K) and at vacuum wavelengths in the spectral range 244 to 346 nm, measured by means of Fourier-Transform Spectroscopy (FTS) at DLR at a spectral resolution of 3.3 cm^{-1} (0.02-0.04 nm). A total of 191 measurements were recorded in two spectral ranges. Absorption cross-sections were obtained at each temperature by means of a global least squares fit. Below 285.71 nm, absorption cross-sections were smoothed to 7.7 cm^{-1} (0.04-0.06 nm) resolution by convolving with a Gaussian to reduce the noise. Offset corrections were made for each of the 6 temperatures by fitting to the SER dataset (constant for all wavelengths) since it was measured at higher ozone column density and thus considered more reliable regarding offset. After offset correction polynomials of 1st order (<270.27 nm) ~~>~~ and 2nd order (>270.27 nm) in temperature were fitted for each spectral point to improve the statistical uncertainty. The offset corrections have a minor effect on the cross-sections except for wavelengths above ~330 nm. Figure 1.a illustrates BW measurements without polynomial fit in temperatures to be fairly compared with BDM measurements (Fig. 1.b) with respect to the dependence of cross-sections on wavelength and temperature. The BDM measurements are given at five temperatures (218, 228, 243, 273, and 295 K) and at air wavelengths over the spectral range 195-519 nm with spectral resolution of 0.01-0.02 nm. Note that the wavelengths of these measurements are converted to vacuum wavelengths in Figure 1.b~~.~~. Measured cross-sections are typically parameterized quadratically to be applied conveniently at any atmospheric temperature~~s~~ using the following equation:

$$C = C_0 + C_1(T - 273.15K) + C_2(T - 273.15K)^2 \quad (1)$$

This quadratic equation was first found to represent well the temperature dependence of ozone cross

section in the UV (Paur and Bass, 1985) and has now become the standard approach (Liu et al., 2007; 2013; Chehade et al., 2013a;2013b; Serdyuchenko et al., 2014). The non-linear least squares fitting between measured and parameterized spectrum ~~used in this paper~~ converges typically within 3 iterations for both BDM and BW. Measurements at 273 K are excluded for the BDM quadratic temperature fitting, according to Liu et al. (2007). In Figure 2, the derived temperature dependent coefficients are illustrated, with their relative differences. C_o values are similar to each other in the Hartley band (<310 nm) with relative biases of 2-3%. However, the Huggins band (>310 nm) shows large spiky biases of up to 8%. C_1 and C_2 represent linear and quadratic temperature dependences of absorption cross-sections, respectively. The cross-sections in the Hartley band are almost independent of the temperature variation and thereby large differences of these coefficients between two datasets are due the large correlation between C_1 and C_2 and are of minor importance to the parameterized cross-sections. However, the Huggins band shows the distinctly different temperature dependence between the two cross-section datasets, especially for the quadratic terms. For C_2, the BW data show more monotonic wavelength dependence in the range 290-310 nm. Note that we determined that the parameterization schemes used in this work and Birk and Wagner (2018) are very similar by the fact that no residuals remain when comparing BW cross-sections with these two schemes (not shown here). Figure 3 compares the residuals of the fitted cross-sections relative to the original measurements interpolated to many atmospheric temperatures using a spline scheme. The BDM quadratic approximation has large positive residuals of up to 15 % for the temperatures ranging from 243 and 295 K due to insufficient sampling to account for the non-linearity of the temperature dependence, especially for the longer UV wavelength range. Moreover, approximating the BDM cross-sections at temperatures below 218 K results in errors of ± 5% below 315 nm and up to ± 40% above. Compared to the BDM dataset, the parameterization of BW cross-sections results into significantly reduced residuals, of 0.25% below 320 nm and typically less than 2% at longer wavelengths if the temperature is within the boundaries of the measurements. Residuals are within 5% even if the temperatures are out of the boundaries. This demonstrates that the temperatures of BW measurements are well selected to characterize the temperature dependence of ozone cross-sections, whereas there are cross-section errors due to the BDM parameterization ~~exist~~. Figure 4 shows the direct comparison of parameterized cross-sections between BDM and BW. The difference of cross-sections between BDM and BW are generally consistent with the corresponding comparison of C_0 around 270 K. The differences at different temperatures are typically within 2% for wavelengths below 310 nm except for several spikes around 276, 297, and 306 nm that are correlated with the differences of C_2. At wavelengths larger than 315 nm, the inconsistency between BDM and BW ~~biases~~ shows large temperature dependence, with the ~~bias~~ differences ~~range~~ increasing from ~5% at 315 nm to ~20% at 340 nm.

3. Impact of using different cross sections on ozone profile retrievals

OMI ozone profiles are retrieved at 24 layers from BUV spectra for 270-309 nm in UV1 and 312-330 nm in UV2 using an optimal estimation technique (Liu et al. 2010). The ~~implemented~~ configurations implemented in this work are similar to those in Liu et al. (2013). One orbit of measurements on 1th July 2006 is used to see how our retrievals are changed due to using different cross-sections. Figure 5 shows the response of our retrievals to the parameterization errors shown in Figure 3 as functions of solar zenith angle (SZA). Compared to the BDM, the ozone retrievals are almost independent of the BW parameterization errors, with individual differences of 2-3% below 20 km and ~0% above. The differences of the BDM cross-sections with and without the parameterization are -5 to 15% in the lower troposphere at smaller SZAs and up to ± 20% around 10 km at higher SZAs. The UV photon penetration down to the lower atmosphere decreases with SZAs increasing and thereby tropospheric ozone retrievals become insensitive due to cross-section errors at high SZAs, while a priori ozone information becomes more important to the retrieval. Figures 6-8 show the retrieval differences when parameterized BW and BDM cross-sections are implemented, respectively. To evaluate the different implementations, both fitting and retrieval accuracies are assessed. However, it is very hard to see large differences in fitting residuals at the final iteration compared to differences ~~on~~ of the retrieved elements of the state vector because the algorithm iteratively updates the state vector toward minimizing the differences in the spectral residuals. The fitting residuals are comparable at final iteration when applying BW and BDM dataset as shown in Figure 6.a except for noticeable smaller residuals ~~in~~ for 310-320 nm. However, we can find ~~the~~ distinct changes in the mean residuals of measured radiance to simulated radiance at the initial iteration, mainly over the wavelength range ~~of~~ 290 to 315 nm, up to 5 % as shown in Figure 6.b. On the other hand, Liu et al. (2007, 2013) demonstrated the distinct change of final fitting residuals when changing BDM to BP and GMFM, implying that using BW dataset improves fitting accuracies over using BP and GMFM, but produces similar fitting accuracies to using BDM and SER. ~~-~~Figure 7 shows both relative and absolute differences of the retrieved ozone profiles with the corresponding temperature profiles taken from the National Centers for Environmental Protection (NCEP) final (FNL) operational global analysis data. ~~Large~~ D~~d~~ifferences of 20-50% commonly exist along the tropopause, where the original BDM measurements could not cover atmospheric temperatures below 218 K (Fig. 7a). Some larger differences occur throughout the troposphere in the tropics likely due to the relatively smaller retrieved partial ozone columns. The individual differences of retrieved ozone in the lower troposphere are ~ 20%. However, the corresponding impact on the total column ozone~~,~~ from integrating retrieved ozone profiles ~~are~~is overwhelmed by the stratospheric layers (20-30 km), as shown in Fig. 7b, where the ozone amount is relatively large and the dependence of ozone-cross sections on ~~the~~ temperature is still important. ~~Corresponding differences of total column ozone, from~~

~~integrating retrieved ozone profiles, are also presented by the black line in Fig. 7a.~~ As a result, ~~Applying~~ applying BDM causes an underestimation of total ozone except at the South Pole due to the biggest inconsistency of two cross-sections at the coldest temperature just above the tropopause in spite of smaller amount of ozone compared to upper stratospheric layers~~, despite the overestimation being prominent for the individual layer columns in the troposphere~~. The magnitude of this underestimation/overestimation is ~1 %, which is comparable to the overall accuracy (~1.5%) of the OMI operational total ozone product against ground-based measurements (McPeters et al., 2015). The wavelength shifts between ozone cross-sections and radiances are iteratively and simultaneously fitted with ozone for their respective UV1 and UV2 channels. Figure 8 compares how the wavelengths of different cross-sections are adjusted in each fitting window at nadir view. According to Schenkeveld et al. (2017), wavelength errors of OMI radiances are expected to be ~0.002 nm in UV2 and ~0.015 nm in UV1. The fitted wavelength shifts fall in the ranges of the OMI wavelength accuracy. Compared to the BDM, the BW dataset has the relative shifts of ~0.002 nm in the UV2. The mean shifts in the UV1 are comparable, 0.0087 nm and 0.0081 nm for BDM and BW, respectively, whereas the variance of the fitted shifts over the latitude is reduced with the use of BW dataset as the shifts are more stable south of 30°S. On the other hand, Liu et al. (2013) shows that the relative shifts between SER and BDM are ~ 0.007 nm in both UV1 and UV2, and BP shifts vary largely with latitude by up 0.01 nm. These results indirectly demonstrate the similarity of the wavelength calibration quality between BDM and BW measurements.

4. Validation with ozonesonde observations

Ozonesonde measurements at five stations during the period 2005 to 2008 are used to evaluate the retrieval accuracy of ozone profile retrievals using different cross-sections. In addition to the currently used BDM and the new BW datasets, BP and SER previously assessed in Liu et al. (2013) are included in this evaluation. Typically, high-resolution vertical structures of ozonesonde profiles (~100 m) are degraded to OMI resolution (6-10 km in the stratosphere, 10-15 km in the troposphere) using retrieval averaging kernels to eliminate the effect of OMI smoothing errors (80% of total retrieval errors in the lower stratosphere and troposphere) in comparison with ozonesondes; as a result, the standard deviations of comparisons are typically reduced by a factor of 2 in the troposphere and lower stratosphere while the comparisons of mean biases are less impacted by using OMI smoothing errors or not. In this paper, the conclusion on which cross-section data should be used stays the same no matter whether ozonesonde profiles are vertically smoothed or not, so we present validation results only using original ozonesonde measurements. In Figure 9, mean biases of the retrieved ozone profiles relative to ozonesondes and the corresponding standard deviations are presented at each station, arranged ~~by~~ in latitude from north to south, together with corresponding

ozonesonde ozone profiles and temperature profiles.

In layers above ~20 km, a negligible impact of using different cross-sections is found because the measurement information comes mainly from the Hartley ozone absorption band with little dependence on temperature variation. Both BP and SER measurements provide a wider temperature range and more samplings than BDM, but switching from BDM to BP / SER results in large altitude-dependent oscillations of mean biases below ~20 km and noticeably fewer successful retrievals, consistent with Liu et al. (2013). These oscillations tend to be wider with the minimum atmospheric temperatures, decreasing such that the mean biases increase ±50% at mid/high latitudes (210-215 K) to ±70% at low latitudes (200-205 K), which is partly due to smaller ozone concentration in the tropics and hence the larger relative differences. This result implies a defect in accounting for the temperature dependence in both the BP/SER cross-section datasets, especially in the lower temperature range. Using BDM and BW cross-sections generally show much smaller altitude-dependent oscillations of mean biases. The magnitudes of the biases are smaller for BDM for the two middle/high latitude stations, but smaller for BW at the other, lower latitude, stations. The BW retrievals typically show negative biases of up to 30% relative to BDM retrievals. The number of successful BW retrievals is slightly smaller than that of BDM retrievals because the negative biases cause more occurrences of negative ozone so that the retrieval convergence is more difficult. It is difficult to determine which one is better for ozone profile retrievals from the mean biases as OMI radiances contain systematic radiometric calibration errors (Liu et al., 2010) and ozonesonde observations can also contain systematic measurement errors (Liu et al., 2006).

As seen from the comparison of standard deviations in the middle panels, the use of BW consistently gives significantly smaller standard deviations, by 5-20% in the lower stratosphere and upper troposphere except for the high latitude station, Sodankyla. BW, BDM, and SER retrievals show similar standard deviations at this station probably due to relatively warmer temperature, ~210-220 K in this altitude range. In Figure 10, individual differences of layer column ozone between OMI retrievals and ozonesondes using BDM and BW datasets are plotted as a functions of temperatures for 8 layers below ~20 km. In this comparison, the noticeable reduction of the scatter between OMI and ozonesonde, by 5-15% at layers from 17 to 8.5 km as well as by a few % below or above them, after applying BW cross-sections is further evident. Improvements of the retrieval precision, corresponding to standard deviations, have been less often achieved than those of the retrieval accuracy corresponding to mean biases; for examples, systematic errors in ozone profile retrievals could be reduced by accounting for polar mesospheric clouds (Bak et al. 2016) and slit function errors (Bak et al. 2019) as well as applying empirical calibration (Bak et al. 2017) whereas the reduction of the standard deviations was achieved only in Bak et al. (2013) by better representing

dynamically induced ozone variability in the a priori ozone. This significant improvement in standard deviations indicates that temperature dependence is better characterized at the lower temperatures near ~200K by the BW dataset.

5. Summary and discussion

This paper evaluates the recently measured laboratory high-resolution BW (2018) ozone cross-section data within the framework of the ESA project SEOM-IAS to see whether or not the current recommendation ~~could~~ should be changed for improving ozone profile retrievals from UV measurements. The BDM (1993) dataset has been regarded as the standard ozone absorption cross-section in space-based ozone profile retrievals from BUV measurements: thereby we focused on comparing BW and BDM datasets and their impact on our ozone profile retrievals from OMI BUV measurements. Compared to BDM, given at 5 temperatures ranging from 218 to 295 K, the BW dataset provides improved temperature coverage of 193 to 293 K, every 20 K. To conveniently apply the cross-section measurements at any temperature, we quadratically parameterized its temperature dependence using iterative non-linear least squares fitting. The 273 K measurements are excluded in the BDM parameterization to improve the fitting residuals at other temperatures. However, the BDM parameterization causes increasing ~~biases~~ fitting residuals in approximate cross-sections at lower temperatures using their 243 and 218 K measurements, especially at longer wavelengths in the Huggins band (up to 20%). It reveals serious errors of up to ± 40% in representing the values at lower temperatures out of the BDM measurements. In comparison, the BW approximation is very closely parameterized to the original data, typically within 2%, while most of the atmospheric temperatures are covered by the BW dataset; the ~~biases~~ residuals increase to ±5% at temperatures below 195 K. Correspondingly, individual ozone profile retrievals show less sensitivity ~~due to~~to the BW parameterization errors, with ~~biases~~ differences of ~ 2% or less over the altitude range. On the other hand, using the parameterized BDM causes ~~biases~~ an overestimation of 5-10% at bottom layers in the low latitudes and 10-20% at the tropopause. Relative to the BDM dataset, the BW data show systematic ~~biases~~ differences of 2-3% in the cross section at ~~0°C~~273K (C_o) at shorter wavelengths below 300 nm, but larger spikey ~~biases~~ differences of up to 8% at wavelengths longer than 315 nm. The differences in C_1 and C_2 ~~implies~~ imply a distinctly different temperature dependence especially in non-linearity in the Huggins bands. We then compared ozone profile retrievals from one orbit of OMI measurements with BW and BDM cross-section datasets. Using different datasets gives comparable results in the wavelength shifts of cross-sections relative to OMI radiance wavelengths and fitting residuals at the final iteration, respectively. However, the initial

iteration gives ~5% differences in fitting residuals near 290-315 nm, which results in significant differences of the adjusted ozone profiles at the final iteration, ~50% at the tropopause across most latitudes and ~20% at the bottom layers in the low-latitudes. To evaluate the quality of ozone retrievals, ozonesonde measurements are compared at five stations. In this validation, we include other cross-section datasets, BP (1985) and SER (2014). Compared to the large vertical oscillation of mean biases for OMI ozone profiles using BP and SER, the BW retrievals show mean biases comparable to or sometimes improved over the BDM retrievals. The most important improvement due to switching from BDM to BW is the significant reduction of the standard deviations, by up to 15% in the lower stratosphere and upper troposphere where atmospheric temperatures are lower than ~200 K.

Based on this evaluation, switching our ozone absorption cross-section reference from BDM to BW is very promising for OMI ozone profile retrievals. However, in this evaluation soft calibration is turned off and thereby the final decision on our algorithm will be made after further evaluating our retrievals with BW-based soft calibration. In order to make a robust recommendation it might be useful for the ACSO committee to organize another activity to assess the impact of applying this new dataset on other ozone measurements on column ozone or profiles from various platforms. The results of this work in addition to that of Orphal et al. (2016) will help the HITRAN committee to decide which cross-sections should be included in HITRAN2020 edition.

Using different ozone cross-sections could also cause an important change in SO_2 retrievals fitted in the Huggins band and therefore ~~it~~ the impact of applying both ozone and SO_2 cross-sections available from the BW datasets (https://zenodo.org/record/1492582) should be evaluated. However, the spectral coverage of the BW dataset is insufficient for the spectral fitting of other trace gases such as BrO and HCHO, both of which have significant interference ~~with~~ from ozone. Ozone cross-sections in other wavelength ranges, such as the mid-infrared region near 9.6 μm and the Chappuis band (400-650 nm), have not been thoroughly evaluated in the literature. The ozone profile algorithm used in this work will be implemented for the Tropospheric Emissions: Monitoring of Pollution (TEMPO) satellite combining the UV and visible measurements to improve the detection of boundary layer ozone. Therefore we should extend this work to find the most suitable ozone cross-sections in the TEMPO visible ozone channel (540-740 nm), focusing on SER 2014 covering from 213 to 1100 nm (193-293 K in 10K steps) and that of Brion et al. (1998) which provides measurements at 218 and 295 K from ~520 nm to ~650 nm. Moreover, the need to improve wide spectral range laboratory cross-section measurements of ozone is still required to advance atmospheric ozone and other trace gases measurements.

Author contributions. JB and XL designed the research; MB, GW, and IG contributed to oversight and guidance

for ozone cross-sections; JB conducted the research and wrote the paper; XL and KC contributed to analysis and writing.

Competing interests. The authors declare that they have no conflicts of interest.

Data availability, The BW cross-section dataset is available at https://zenodo.org/record/1485588. OMI Level1b radiance datasets are available at https://aura.gesdisc.eosdisc.nasa.gov/data/Aura_OMI_Level1/ (last access: 31 Nov 2019). The ozonesonde data used to validate our ozone profile retrievals were obtained though the WOUDC and SHADOZ. The WOUDC dataset is available at https://woudc.org/data/products/ozonesonde/(last access: 31 Nov 2019) and for the SHADOZ dataset at https://tropo.gsfc.nasa.gov/shadoz/Archive.html (last access: 31 Nov 2019).

Acknowledgement, We acknowledge the OMI science team for providing their satellite data and the WOUDC and SHADOZ networks for their ozonesonde datasets. Research at the Smithsonian Astrophysical Observatory by Juseon Bak, Xiong Liu, and Kelly Chance was funded by the NASA Aura science team program (NNX17AI82G). MB and GW thank the European Space Agency (ESA) for funding of the SEOM-IAS project (ESA/AO/1-7566/13/I-BG).

Financial support. This research has been supported by NASA Aura science team program (grant no. NNX17AI82G). The SEOM-IAS project has been funded by ESA (ESA/AO/1-7566/13/I-BG).

References

Bak, J., Liu, X., Kim, J. H., Deland, M. T., and Chance, K.: Improvement of OMI ozone profile retrievals by simultaneously fitting polar mesospheric clouds, Atmos. Meas. Tech., 9, 4521–4531, https://doi.org/10.5194/amt-9-4521-2016, 2016.

Bak, J., Liu, X., Kim, J.-H., Haffner, D. P., Chance, K., Yang, K., and Sun, K.: Characterization and correction of OMPS nadir mapper measurements for ozone profile retrievals, Atmos. Meas. Tech., 10, 4373–4388, https://doi.org/10.5194/amt-10-4373-2017, 2017

Bak, J., Liu, X., Sun, K., Chance, K., and Kim, J.-H.: Linearization of the effect of slit function changes for improving Ozone Monitoring Instrument ozone profile retrievals, Atmos. Meas. Tech., 12, 3777–3788, https://doi.org/10.5194/amt-12-3777-2019, 2019.

Bak, J., Liu, X., Wei, J. C., Pan, L. L., Chance, K., and Kim, J. H.: Improvement of OMI ozone profile retrievals in the upper troposphere and lower stratosphere by the use of a tropopause-based ozone profile climatology, Atmos. Meas. Tech., 6, 2239–2254, doi:10.5194/amt-6-2239-2013, 2013.

Bass, A. M. and Paur, R. J.: The ultraviolet cross-sections of ozone. I. The measurements, ~~II — Results and temperature dependence,~~ in: Atmospheric ozone; Proceedings of the Quadrennial, 1, 606–~~616~~610, 1985.

Birk, M. and Wagner, G.: ESA SEOM-IAS – Measurement and ACS database O3 UV region (V ersion I) [Data set]. Zenodo. http://doi.org/10.5281/zenodo.1485588, 2018.

Birk, M., Wagner, G., Gordon, I. E., & Drouin, B. J.: Ozone intensities in the rotational bands. Journal of Quantitative Spectroscopy and Radiative Transfer, 226, 60–65. https://doi.org/10.1016/J.JQSRT.2019.01.004, 2019

Brion, J, Chakir, A., Charbonnier, J., Daumont, D., Parisse, C., Malicet, J.: Absorption spectra measurements for the ozone molecule in the 350–830 nm region, J. Atmos. Chem. 30 (1998) 291–99, 1998.

Brion, J., Chakir, A., Daumont, D., Malicet, J., and Parisse, C.: High-resolution laboratory absorp tion cross section of O3. Temperature effect, Chem. Phys. Lett., 213, 610–612, 1993.

Burrows, J. P., Dehn, A., Deters, B., Himmelmann, S., Richter, A., Voigt, S., and Orphal, J.: Atmospheric remote-sensing reference data from GOME: Part 2. Temperature-dependent absorption cross-sections of O3 in the 231–794 nm range, J. Quant. Spectrosc. Radiat. Transfer, 61(4), 509–517, 1999Chehade, W., Gür, B., Spietz, P., Gorshelev, V., Serdyuchenko, A., Burrows, J. P., and Weber, M.: Temperature dependent ozone absorption cross section spectra measured with the GOME-2 FM3 spectrometer and first application in satellite retrievals, Atmos. Meas. Tech., 6, 1623–1632, doi:10.5194/amt-6-1623-2013, 2013a.

Chehade, W.,, Gorshelev, V., Serdyuchenko, A., Burrows, J. P., and Weber, M.: Revised temperature-dependent ozone absorption cross-section spectra (Bogumil et al.) measured with the SCIAMACHY satellite spectrometer, Atmos. Meas. Tech. 6, 3055–3065, http://dx.doi.org/10.5194/amt-6-3055-2013.2013b

Daumont, Brion, J., Charbonnier, J., and Malicet, J.: Ozone UV spectroscopy I: Absorption crosssections at room temperature, J. Atmos. Chem., 15, 145–155, 1992.

Gordon, I., Rothman, L., Hill, C., Kochanov, R., Tan, Y., Bernath, P., Birk, M., Boudon, V., Campargue, A., Chance, K., Drouin, B., Flaud, J.-M., Gamache, R., Hodges, J., Jacquemart, D., Perevalov, V., Perrin, A., Shine, K., Smith, M.-A., Tennyson, J., Toon, G., Tran, H., Tyuterev, V., Barbe, A., Császár, A., Devi, V., Furtenbacher, T., Harrison, J., Hartmann, J.-M., Jolly, A., Johnson, T., Karman, T., Kleiner, I., Kyuberis, A., Loos, J., Lyulin, O., Massie, S., Mikhailenko, S., Moazzen-Ahmadi, N., Müller, H., Naumenko, O., Nikitin, A., Polyansky, O., Rey, M., Rotger, M., Sharpe, S., Sung, K., Starikova, E., Tashkun, S., Auwera, J. V., Wagner, G., Wilzewski, J., Wcisło, P., Yu, S., and Zak, E.: The HITRAN2016 molecular spectroscopic database, J. Quant. Spectrosc. Ra~~.,~~ diat. Transfer, 203, 3–69, https://doi.org/10.1016/j.jqsrt.2017.06.038, 2017.

Gorshelev, V., Serdyuchenko, A., Weber, M., Chehade, W., and Burrows, J.P.: High spectral resolution ozone absorption cross-sections – Part 1: Measurements, data analysis and comparison with previous measurements around 293 K, Atmos. Meas. Tech., 7, 609–624, doi:10.5194/amt-7-609-2014, 2014.

Hearn, A. G.: The absorption of ozone in the ultra-violet and visible regions of the spectrum. Proceedings of the Physical Society, 78(5), 932–940. https://doi.org/10.1088/0370-1328/78/5/340, 1961.

Hodges, J. T., Viallon, J., Brewer, P. J., Drouin, B. J., Gorshelev, V., Janssen, C., ~~et al.~~Lee, S., and Possolo, A. : Recommendation of a consensus value of the ozone absorption cross-section at 253.65 nm based on a literature review. Metrologia, 56(3), https://doi.org/10.1088/1681-7575/ab0bdd, 2019

McPeters, R. D., Frith, S., and Labow, G. J.: OMI total column ozone: extending the long-term data record, Atmos. Meas. Tech., 8, 4845–4850, https://doi.org/10.5194/amt-8-4845-2015, 2015.

Liu, C., Liu, X, and Chance, K.: The impact of using different ozone cross sections on ozone profile retrievals from OMI UV measurements, J. Quant. Spectrosc. Ra., 130, 365–372, doi:10.1016/j.jqsrt.2013.06.006, 2013.

Liu, X., Bhartia, P.K, Chance, K, Spurr, R.J.D., and Kurosu, T.P.: Ozone profile retrievals from the ozone monitoring instrument. Atmos. Chem. Phys., 10, 2521–2537, 2010.

Liu, X., Chance, K., Sioris, C. E., and Kurosu, T. P.: Impact of using different ozone cross sections on ozone profile retrievals from Global Ozone Monitoring Experiment (GOME) ultraviolet measurements, Atmos. Chem. Phys., 7, 3571–3578, doi:10.5194/acp-7-3571-2007, 2007.

Liu, X., Chance, K., Sioris, C. E., and Kurosu, T. P, Newchurch, M.J.: Intercomparison of GOME, ozonesonde, and SAGE II measurements of ozone: Demonstration of the need to homogenize available ozonesonde data sets, J. Geophys. Res. 111 (D14) D14305, doi:10.1029/2005JD006718, 2006..

Liu, X., Chance, K., Sioris, C. E., Spurr, R. J. D., Kurosu, T. P., Martin, R. V., and Newchurch, M. J.: Ozone profile and tropospheric ozone retrievals from Global Ozone Monitoring Experiment: algorithm description and validation, J. Geophys. Res., 110, D20307, doi: 10.1029/2005JD006240, 2005.

Malicet, Daumont, D., Charbonnier, J., Parisse, C., Chakir, A., and Brion, J.: Ozone UV spectros copy. II. Absorption cross-sections and temperature dependence, J. Atmos. Chem, 21, 263–27 3, 1995.

Rothman, L. S., Jacquemart, D., Barbe, A., Chris Benner, D., Birk, M., Brown, L. R., et al.: The HITRAN 2004 molecular spectroscopic database. *Journal of Quantitative Spectroscopy and Radiative Transfer*, *96*(2), 139–204. https://doi.org/10.1016/j.jqsrt.2004.10.008, 2005.

Paur, P. J. and Bass, A. M.: The ultraviolet cross-sections of ozone: II. Results and temperature dependence, in Atmospheric Ozone, in: C.S. Zerefos, A. Ghazi (Eds.), Proceedings of the Quadrennial Ozone Symposium 1984, pp. 611–615. Dordrecht Reidel, Norwell, MA., 1985

Schenkeveld, V. M. E., Jaross, G., Marchenko, S., Haffner, D., Kleipool, Q. L., Rozemeijer, N. C., Veefkind, J. P., and Levelt, P. F.: In-flight performance of the Ozone Monitoring Instru ment, Atmos. Meas. Tech., 10, 1957–1986, https://doi.org/10.5194/amt-10-1957-2017, 2017.

Seo, S., Richter, A., Blechschmidt, A.-M., Bougoudis, I., and Burrows, J. P.: First high-resolution BrO column retrievals from TROPOMI, Atmos. Meas. Tech., 12, 2913–2932, https://doi.org/10.5194/amt-12-2913-2019, 2019.

Serdyuchenko, A., Gorshelev, V., Weber, M., Chehade, W., and Burrows, J. P.: High spectral resolution ozone absorption cross-sections – Part 2: Temperature dependence, Atmos. Meas. Tech., 7, 625–636, https://doi.org/10.5194/amt-7-625-2014, 2014.

Orphal, J.: A critical review of the absorption cross-sections of O3 and NO2 in the 240–790 nm region, Part 1. ozone, in ESA Technical Note MO-TN-ESA-GO-0302, ESA-ESTEC, Noordwijk, The Netherlands, 2002.

Orphal, J.: A critical review of the absorption cross-sections of O3 and NO2 in the 240–790 nm region, J. Phtotochem. Photobiol. A., 157, 185–209, 2003.

Orphal, J., Staehelin, J., Tamminen, J., et al.: Absorption crosssections of ozone in the ultraviolet and visible spectral regions: Status report 2015, J. Mol. Spectrosc., 327, 105–121, https://doi.org/10.1016/j.jms.2016.07.007, 2016.

Theys, N., De Smedt, I., Yu, H., Danckaert, T., van Gent, J., Hörmann, C., Wagner, T., Hedelt, P., Bauer, H., Romahn, F., Pedergnana, M., Loyola, D., and Van Roozendael, M.: Sulfur dioxide retrievals from TROPOMI onboard Sentinel-5 Precursor: algorithm theoretical basis, Atmos. Meas. Tech., 10, 119–153, https://doi.org/10.5194/amt-10-119-2017, 2017.

Tyuterev, V. G., Barbe, A., Jacquemart, D., Janssen, C., Mikhailenko, S. N., & Starikova, E. N.: Ab initio predictions and laboratory validation for consistent ozone intensities in the MW, 10 and 5 μm ranges. The Journal of Chemical Physics, 150(18), 184303. https://doi.org/10.1063/1.5089134, 2019.

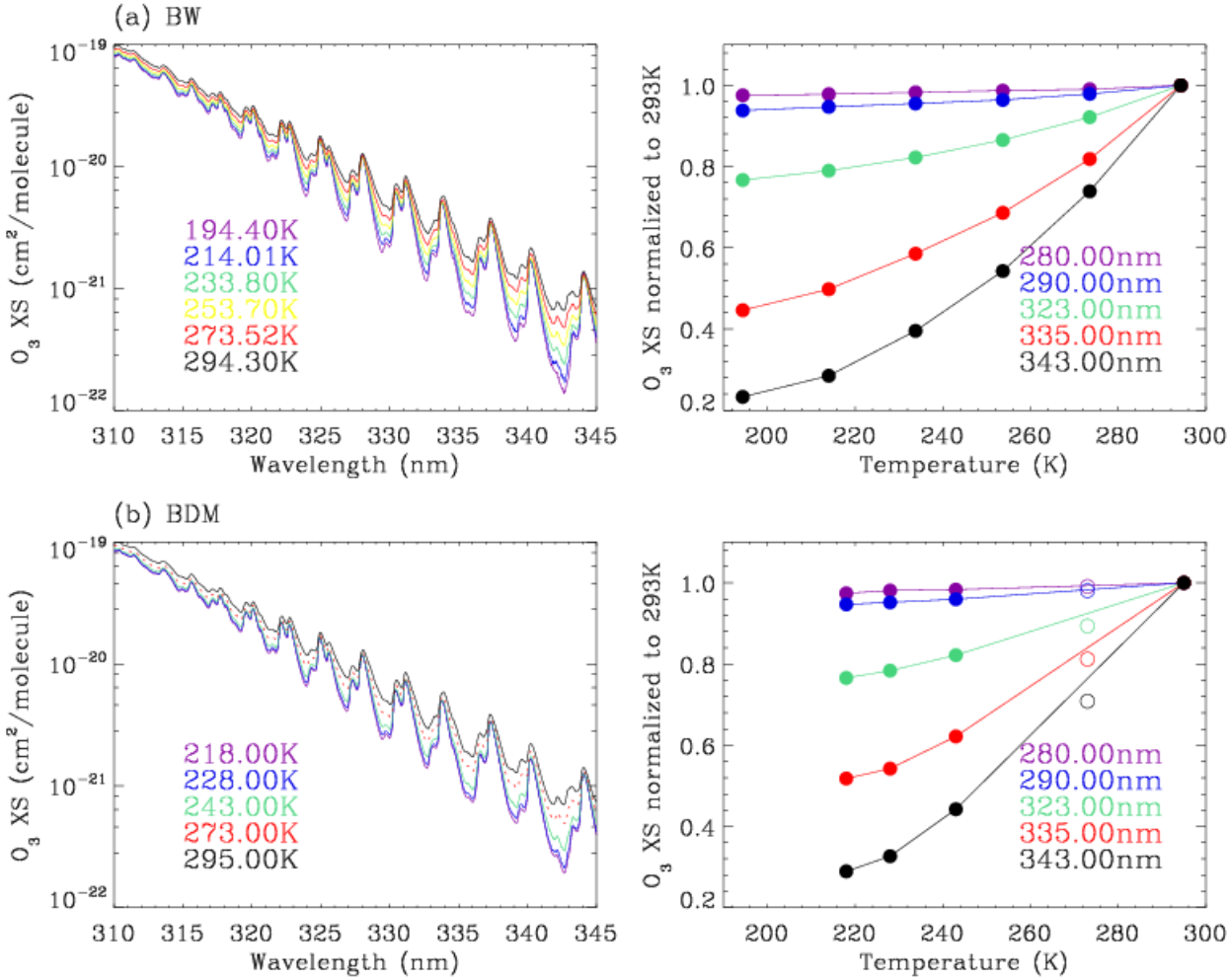

761

762 **Figure 1. (Left) Measurements of ozone absorption cross-sections at all selected temperatures in**
763 **the Huggins bands taken from (a) BW (2018) and (b) BDM (1995), respectively. (Right) For BW,**
764 **the experimental data are plotted without the quadratic parameterization for a fair comparison**
765 **with BDM. BDM measurements at 273 K are plotted with a dotted line on the left and with open**
766 **circles on the right, because the data at this temperature are not recommended for use, by Liu et**
767 **al. (2007).**

768

769

770

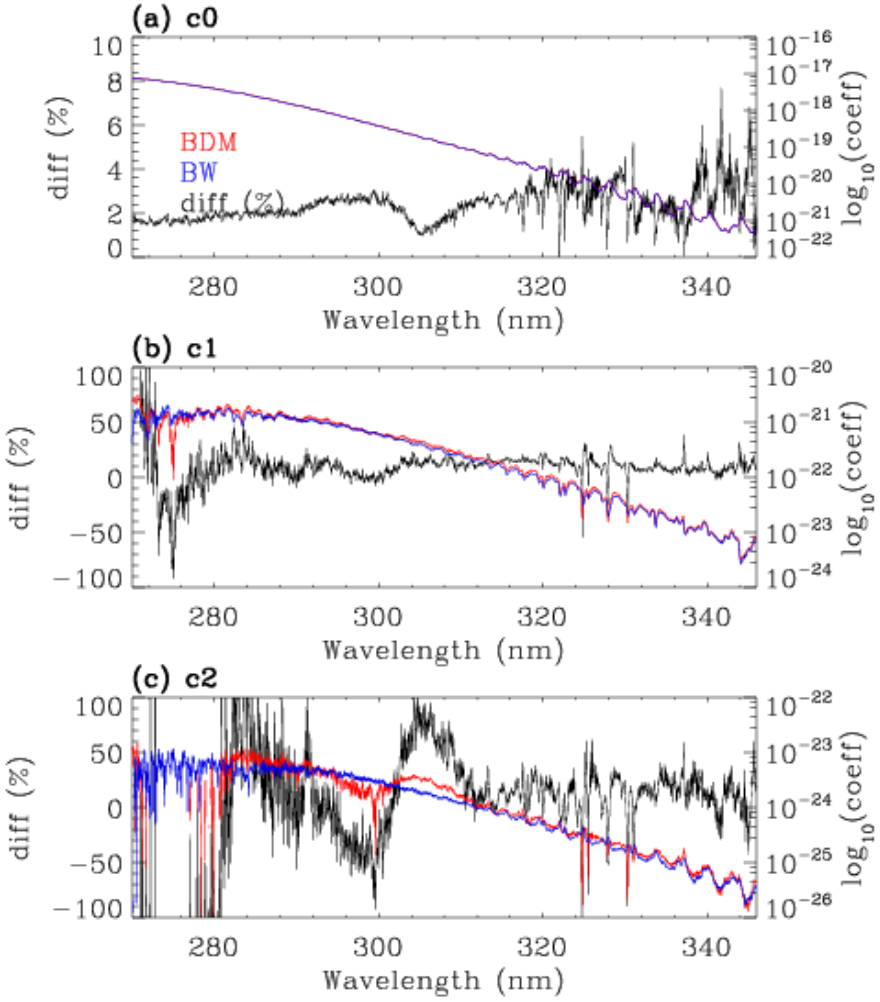

771

772 **Figure 2. Quadratic coefficients (cm^2/molecule) to parameterize the temperature dependence of**
773 **ozone cross-sections for BDM (red) and BW (blue), respectively, with their relative differences**
774 **(BDM-BW)/BW in black.**

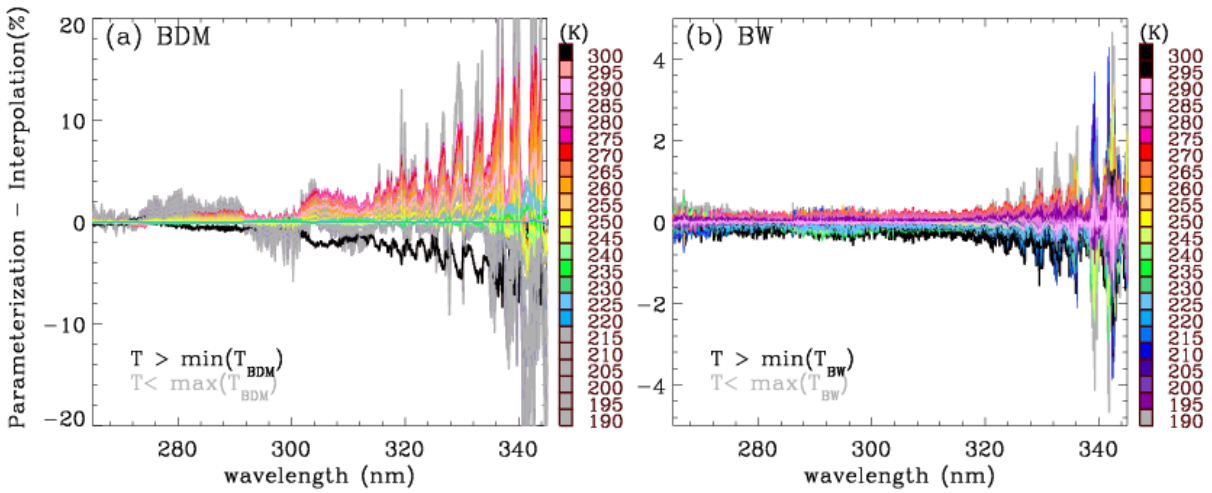

775

776 **Figure 3. Relative differences of ozone cross-sections parameterized and spline interpolated at**
777 **temperatures between 190 and 300 K, for (a) BDM and (b) BW, respectively. In the legend, the**
778 **temperatures not covered by each dataset are indicated with gray and black, for values beyond**
779 **lower and upper boundaries, respectively; so slightly different color scales are ~~actually~~ used in**
780 **these two panels for those outside the measured temperature range.~~.~~**

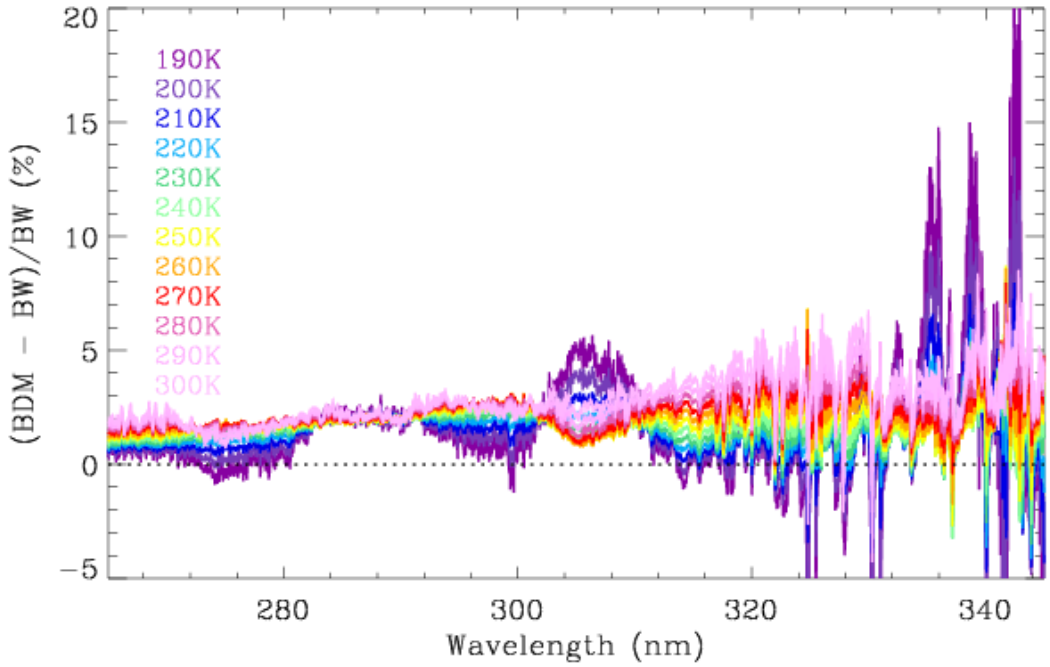

781

782 **Figure 4. Same as Figure 3, but for relative differences (%) of parameterized ozone cross-sections**
783 **~~between~~ of BDM and BW.**

784

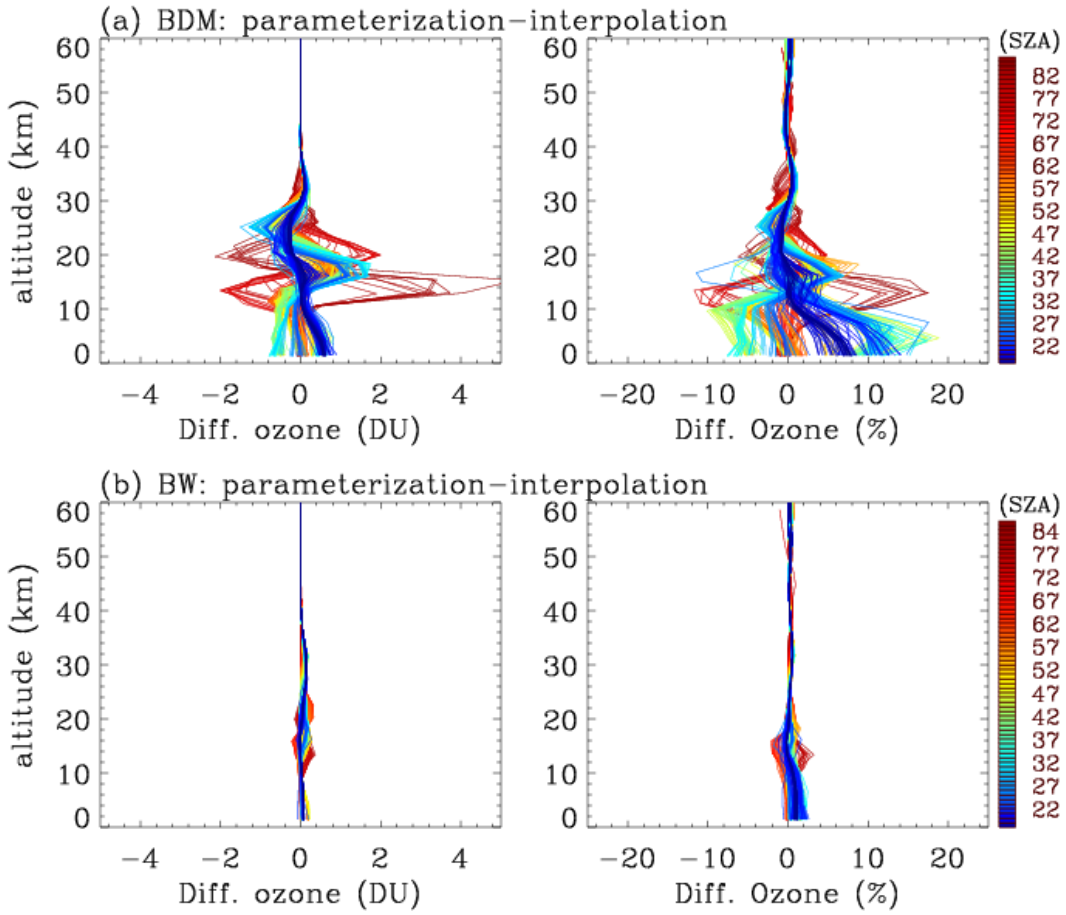

785

786 **Figure 5. The impact of parameterizing the cross-sections shown in Figure 3 on ozone profile**
787 **retrievals, for (a) BDM and (b) BW, as a function of solar zenith angle (SZA). The differences of**
788 **retrieved ozone profiles are assessed in absolute (left panels) and relative (right panels) units,**
789 **respectively.**

790

791

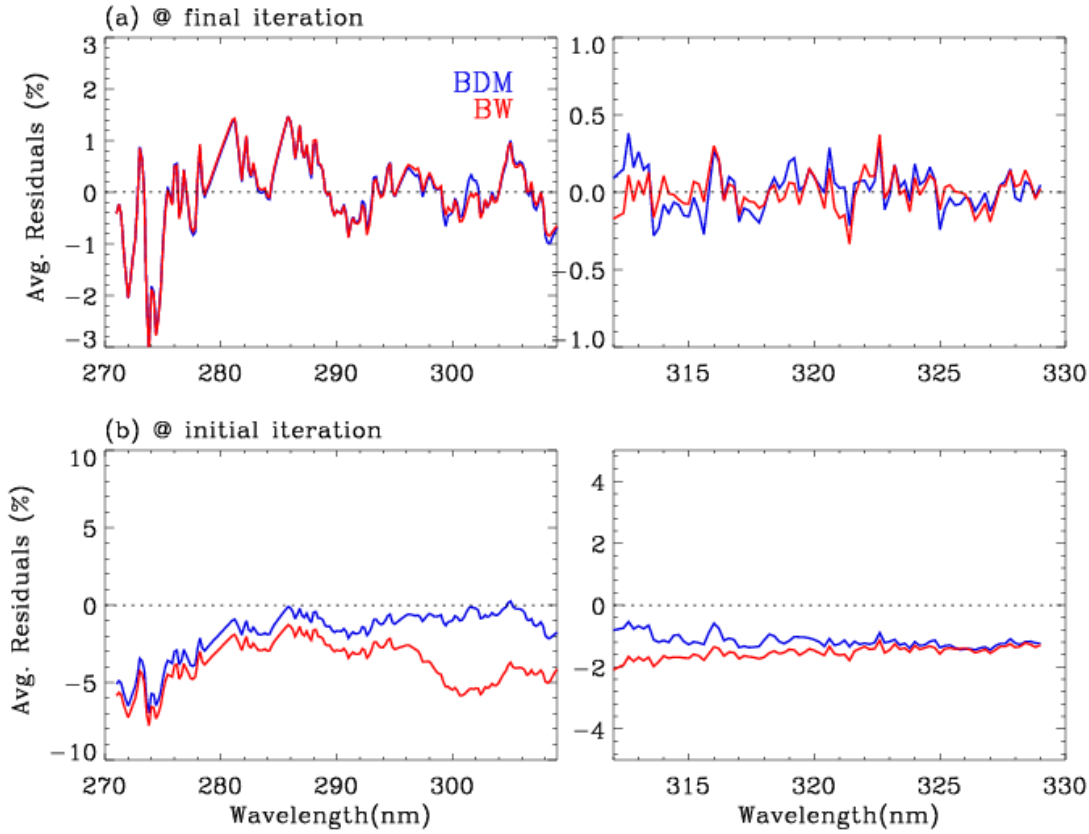

792

793 **Figure 6. Comparison of mean fitting residuals at latitudes of 15° S to 15° N at (a) final iteration**
794 **and (b) initial iteration, respectively, when using BDM (blue) and BW (red).**

795

796

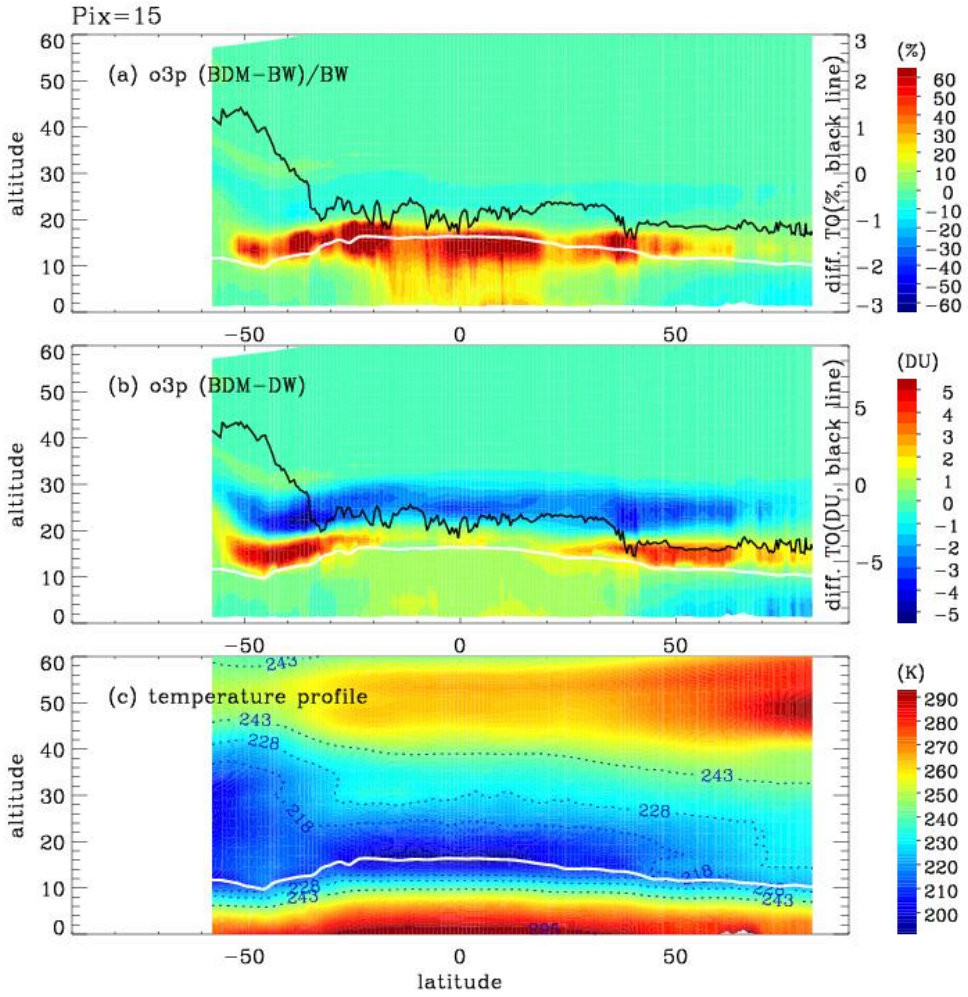

Figure 7. (a) Percent Difference ((BDM-BW)/BW x 100%) of retrieved ozone profiles using BDM and BW datasets at nadir view, (b) absolute differences in the unit of DU and (c) corresponding temperature profiles in the retrievals. In ~~the upper panel~~(ab) and (b), the black line represents the differences of integrated column ozone. The white line in both panels represents the tropopause height.

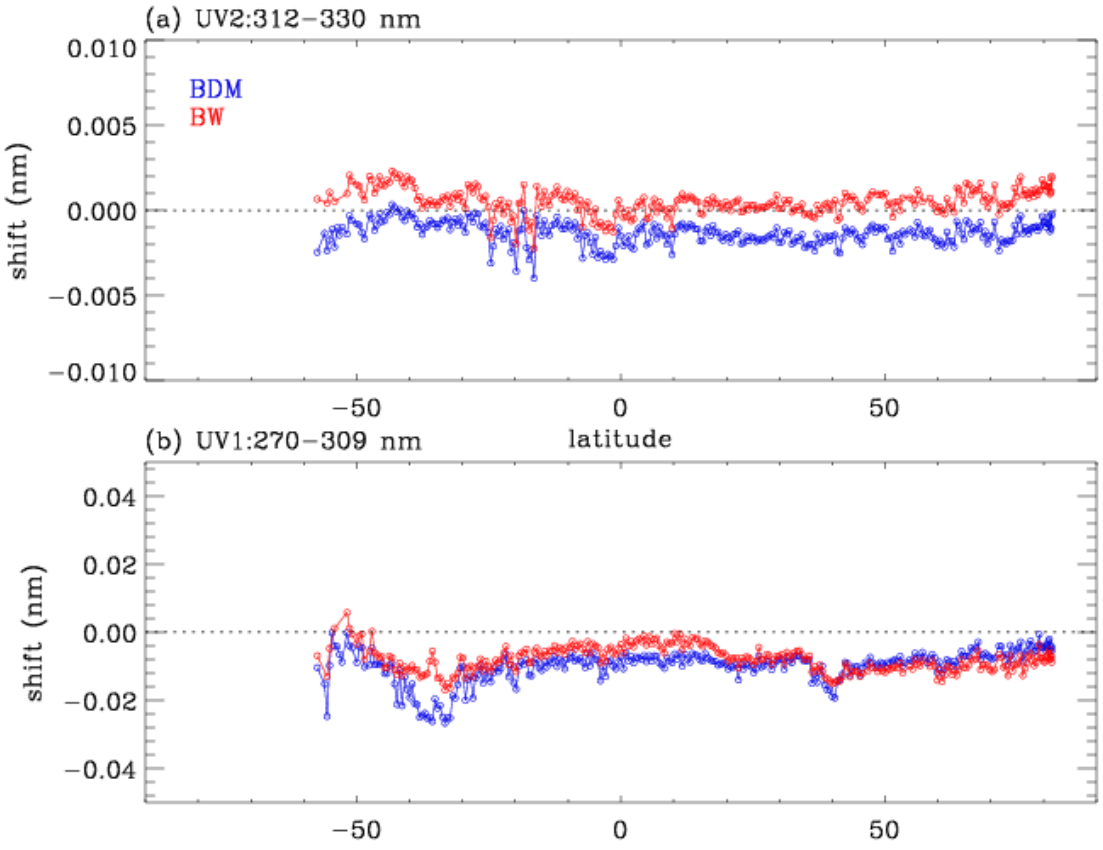

803

804 **Figure 8. Comparison of the wavelength shifts (nm) between ozone cross-sections and OMI**
805 **radiances at the nadir view for using BDM (blue) and BW cross-sections, respectively.**

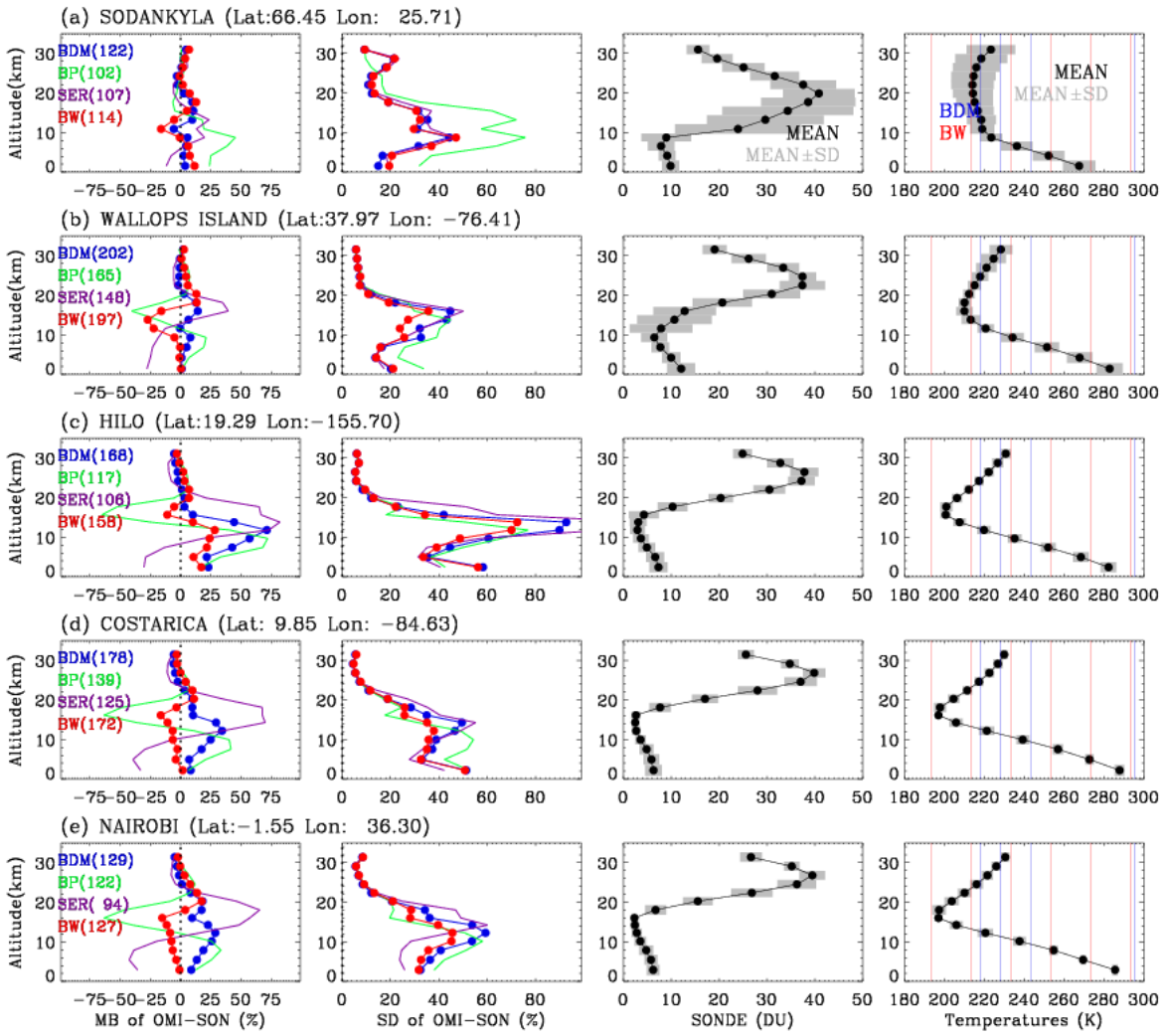

Figure 9. (1st ~~Left~~ column) Mean biases of relative differences between OMI and ozonesonde ozone profiles at five stations arranged with decreasing latitude when four different cross-sections are applied to OMI retrievals, with (~~Middle~~ 2nd column) the corresponding standard deviations ~~and~~. (3th column) ozonesonde and (~~Right~~ 4th column) ~~mean~~ temperatures (black circle) ~~of~~ averaged from individual profiles (gray). The numbers after the four cross-sections in the legends show the number of successful retrievals. Blue and red vertical colors in the ~~right~~ last panels represent the temperatures used to derive the quadratic coefficients from BDM and BW measurements, respectively.

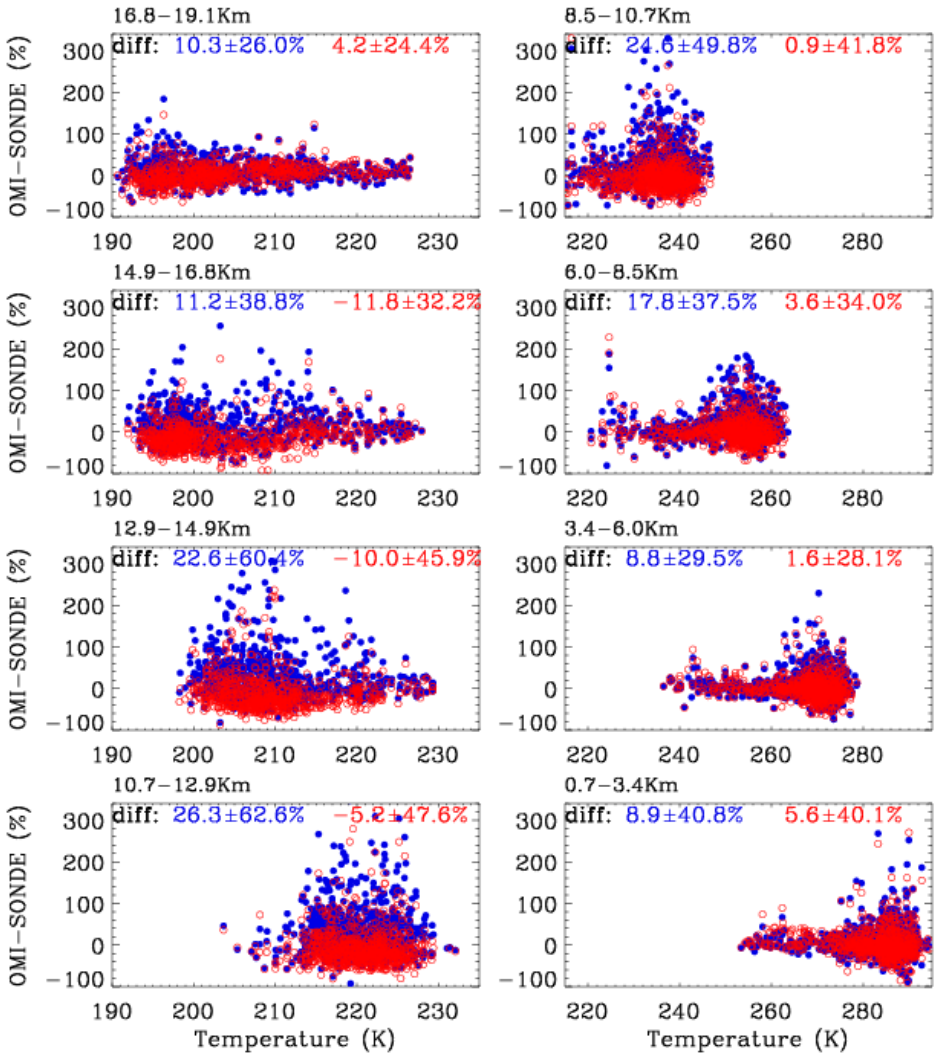

816

817 **Figure 10. Scatter plots of individual differences between OMI retrievals using BDM (blue) and BW**
818 **(red) cross-sections and ozonesonde measurements for each layer from the surface (bottom right)**
819 **to 19.1 km (top left) as functions of layer temperature. Mean differences and standard deviations**
820 **for both cross-sections are shown in the legends.**

821